JOURNAL OF GUIDANCE, CONTROL, AND DYNAMICS
Vol. 23, No. 3, May–June 2000

Optimal Size and Location of Piezoelectric Actuator/Sensors: Practical Considerations

Osama J. Aldraihem*
King Saud University, Riyadh 11421, Saudi Arabia
and
Tarunraj Singh† and Robert C. Wetherhold‡
State University of New York, Buffalo, New York 14260-4400

The problem of obtaining the optimal size and location of piezoelectric actuator/sensors is addressed. An optimization problem is formulated for a general beam that has arbitrary boundary conditions and may have as many piezoelectric actuators as desired. The proposed optimization criterion is based on a beam modal cost and controllability index. If the size of the actuator is unbounded, it frequently is optimal if it covers most, if not all, of the length of the beam. This is not realistic because there are cost, weight, and space factors to be considered. By adding a penalty term to the criterion, the size of the actuator/sensor can be reduced to a practical and reasonable size. Thus, there is no need to preselect the size of the actuator/sensor. The optimal size and location for beams with various boundary conditions are determined for a single pair and for two pairs of actuators. The results are in very good agreement with those reported by other investigators. A comparison is also made between the performance of two pairs of actuators and the performance of a single pair for control of the same number of modes. The improvement in performance with two pairs is quantified.

Nomenclature

a = small and positive constant
b, L = beam width and length, respectively
C = damping matrix
$C_{dx}, C_{d\dot{x}}$ = output influence matrices
c_s = damping coefficient of the beam material
D = control/disturbance influence matrix
d_k, d_{k+1} = beginning and end locations of piezoelectric patch k
d_{31} = piezoelectric coupling coefficient
E = Young's modulus
H = Heaviside step function
K = stiffness matrix
M = mass matrix
P_j = right eigenvectors
Q_V = weighting matrix
q_i = generalized coordinates
R_i = left eigenvectors
T = kinetic energy of the beam
t = thickness
U = potential energy of the beam
V = cost function
v_k = voltage between top and bottom surfaces of each patch of pair k
w = transverse deflection of the beam centerline
y_d = beam output response
α = objective function
β_i = gross measure of controllability
γ = scaling fraction; $0 < \lambda < 1$
δ_{ij} = Kronecker delta
δW_{nc} = virtual work
$\boldsymbol{\eta}$ = modal coordinates vector
θ_{ij} = measure of controllability of ith mode by jth actuator
ρ = mass density
ϕ_i = assumed mode shapes
ω_i = natural frequencies

Subscripts

c = composite
h = host beam
p = piezoelectric patch

Superscripts

$\cdot$ = $\partial(\cdot)/\partial t$
$\prime$ = $\partial(\cdot)/\partial x$

Received 20 August 1997; revision received 1 November 1998; accepted for publication 1 September 1999.

*Assistant Professor, P.O. Box 800, Department of Mechanical Engineering; odraihem@ksu.edu.sa.
†Associate Professor, Department of Mechanical and Aerospace Engineering; tsingh@eng.buffalo.edu.
‡Associate Professor, Department of Mechanical and Aerospace Engineering; mecrcw@acsu.buffalo.edu.

Introduction

DISTRIBUTED piezoelectric materials experimentally have proven to be practical in sensing and controlling the vibrations of flexible structures.[1] These materials offer a number of advantages over conventional actuators, for example, low energy consumption, fast response, high efficiency, and compactness. These advantages have encouraged researchers to establish models for flexible structures (plate, beam, shell) that incorporate piezoelectric actuators/sensors.[1–6]

The piezoelectric actuator/sensor has to be of a suitable size and be located appropriately to ensure maximum effectiveness. The problem of finding the optimal size and location of an actuator/sensor is very challenging. The optimal location of the actuator for a particular structure is the position at which the strain energy of the structure is highest.[7] For shape control (static case), the given structure contains one point of maximum strain energy, and so the optimal location is obvious. For vibration control (dynamic case), however, the structure's response is a combination of the contribution of several modes. The highest strain energy for a given mode may be found at more than one point, and the high strain energy locations may be different for different modes. For example, the second bending mode of a pinned–pinned beam structure has two points of high strain energy. These issues indicate the necessity of using patch actuators for the control of flexible structures.

The first authors who addressed the optimization problem in smart structures were Crawley and de Luis.[7] They briefly mentioned the criterion for finding the optimal location of a piezoelectric actuator for a cantilever beam based on the beam strain energy. Baz and Poh[8,9] solved the problem of location optimization of a preselected actuator size. They used beam finite elements to model a cantilever beam and included the mass and the stiffness of the actuator in the model. Devasia et al.[10] proposed three optimization criteria that were controller dependent. The resulting actuator size was large, which ensures high authority but invalidates the assumption that the mass and stiffness of the actuator can be ignored. Further, they only considered the first two modes and restricted themselves to pinned–pinned boundary conditions. Burke and Sullivan[11] examined the optimization problem for determining the location and length of actuators and sensors to achieve desired modal coefficients. The method for the selection of the desired coefficients is not specified, and no effort is made to minimize the actuator area. Sunar and Rao[12] investigated location optimization of a prechosen actuator size. Their example and results were similar to that of Baz and Poh[8,9]; however, Sunar and Rao[12] used plate finite elements. Yousefi-Koma and Vukovich[13] suggested three optimization criteria, two of which were adopted from Devasia et al.[10] Yousefi-Koma and Vukovich[13] increased the number of optimization parameters to three: the length, the width, and the location of the actuator. Despite the inclusion of actuator stiffness, they excluded the actuator mass in the model. Gabbert and Schulz[14] suggested controller-independent criteria based on the strain energy of the beam. The proposed optimal actuator center location was the point at which the strain energy is highest. For simultaneous control of several modes, they weighted the modes of vibration and multiplied them by the slope difference at the end of the actuator to form a new objective function. Nevertheless, they did not mention how to choose the weighting coefficients.

The stiffness and the inertia of the piezoelectric actuator can greatly alter the natural frequencies and can reshape the mode of vibration of the smart structure.[15] Therefore, the inclusion of the actuator's mass and stiffness is necessary for reliable modeling. In this paper, we modify the optimization criterion given by Kim and Junkins[16] for actuator size and location to fit our requirements. Unlike most of the early works, our criterion is independent of the control law and is based on practical consideration. That is, the designer can constrain the size of the actuator and may choose the modes to be damped out and their relative importance. Size constraint of the actuator is important to avoid altering the beam's weight and stiffness. Whereas the cited researchers equally weighted the structural modes, the criterion given here weights the modes based on their contribution to the system output.

In the theory section of this paper, the mathematical model of a beam structure with surface-bonded piezoelectric patches (segments) will be developed. A general procedure for the optimization of location and size of piezoelectric patches is presented considering all possible boundary conditions. To establish the optimization criterion, the modal controllability/observability and the modal cost theories are briefly reviewed. By combining these theories, a realistic optimization criterion is formed. In the section on numerical examples, the optimal size and location of piezoelectric patches are determined for beams with six different geometrical boundary conditions and one or two patches. The results are compared with other authors' results when available.

Theory

Beam Model

Consider a symmetric stepped beam, as shown in Fig. 1, which consists of a host flexible beam of unspecified boundary conditions and p pairs of piezoelectric patches that are perfectly bonded on the top and bottom surface of the host beam. To reduce the number of optimization parameters, the patches are assumed to have equal thickness t_p and width b. The host beam and the piezoelectric patches both possess rectangular cross section and have the same width. It is assumed that the patches are of identical poling direction and can simultaneously sense and actuate the bending vibration, resulting in self-sensing, collocated actuators.[17,18] Because the bonding layers are very thin, their effects on beam dynamics can be neglected.

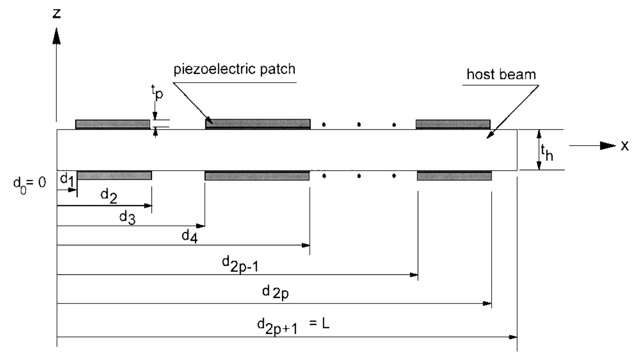

Fig. 1 Geometry of a beam with surface-bonded piezoelectric patches.

To derive the Euler–Bernoulli beam model, the kinetic energy T and the potential energy U of the stepped beam with p patches in bending motion can be expressed as

$$2T = \sum_{k=1}^{p+1} (\rho A)_h \int_{d_{2k-2}}^{d_{2k-1}} \dot{w}^2 \,\mathrm{d}x + \sum_{k=1}^{p} (\rho A)_c \int_{d_{2k-1}}^{d_{2k}} \dot{w}^2 \,\mathrm{d}x \qquad (1)$$

$$2U = \sum_{k=1}^{p+1} (EI)_h \int_{d_{2k-2}}^{d_{2k-1}} (w'')^2 \,\mathrm{d}x + \sum_{k=1}^{p} \int_{d_{2k-1}}^{d_{2k}} \Big\{ (EI)_c (w'')^2 + 2C_p [H(x - d_{2k-1}) - H(x - d_{2k})] \cdot v_k \cdot w'' \Big\} \,\mathrm{d}x \qquad (2)$$

where

$$(\rho A)_h = b\rho_h t_h, \qquad (\rho A)_c = b\rho_h t_h + 2b\rho_p t_p$$

$$(EI)_h = \big(bt_h^3/12\big) E_h, \qquad C_p = bE_p d_{31}(t_h + t_p)$$

$$(EI)_c = (2b/3) E_p \big\{ [t_h/2 + t_p]^3 - (t_h/2)^3 \big\} + \big(bt_h^3/12\big) E_h \qquad (3)$$

where $w(x, t)$ is the transverse deflection of the beam centerline, $v_k(t)$ is the actuation voltage supplied to the pair k, and $H(x - d_i)$, $i = 1, \ldots, 2p + 1$, is the Heaviside step function. The properties ρ_h and E_h and ρ_p and E_p are the host beam and the piezoelectric patches' density and Young's modulus, respectively.

The extended Hamilton's principle is used to derive the equations of motion, that is,

$$\int_{t_1}^{t_2} \delta(T - U) \,\mathrm{d}t + \int_{t_1}^{t_2} \delta W_{\mathrm{nc}} \,\mathrm{d}t = 0 \qquad (4)$$

Because there are no nonconservative forces or moments that are not accounted for in U, the virtual work δW_{nc} is only due to the internal (Kelvin–Voigt) damping of the beam and can be expressed as[19]

$$\delta W_{\mathrm{nc}} = -\int_0^L c_s I \left(\frac{\partial^3 w}{\partial x^2 \partial t} \right) \left(\frac{\partial^2 (\delta w)}{\partial x^2} \right) \mathrm{d}x, \qquad I = \frac{b}{2} \int_z z^2 \,\mathrm{d}z \qquad (5)$$

The assumed modes Rayleigh–Ritz method is the most appropriate approximation method for the optimization problem at hand. The finite element method normally permits only discrete variation of the patch length and location if fixed element sizes were used. In the assumed modes method, the size and the location of the piezoelectric patches can be smoothly changed with no restrictions on the step size. Employing the assumed modes method,[20] the transverse deflection of the beam is approximated as

$$w(x, t) = \sum_{i=1}^{n} \phi_i(x) q_i(t) \qquad (6)$$

where $\phi_i(x)$ is the ith assumed mode shape, $q_i(t)$ is the ith generalized coordinate, and n is the number of terms retained in the approximation.

Substituting Eq. (6) into Eq. (4) and performing the necessary integration leads to

$$M_{ij}\ddot{q}_j + C_{ij}\dot{q}_j + K_{ij}q_j = D_{ik}v_k(t), \qquad i, j = 1, n \tag{7}$$

where the mass, damping, and stiffness matrices are

$$M_{ij} = \sum_{k=1}^{p+1}(\rho A)_h \int_{d_{2k-2}}^{d_{2k-1}} \phi_i\phi_j\,\mathrm{d}x + \sum_{k=1}^{p}(\rho A)_c \int_{d_{2k-1}}^{d_{2k}} \phi_i\phi_j\,\mathrm{d}x$$

$$C_{ij} = \sum_{k=1}^{p+1}(c_sI)_h \int_{d_{2k-2}}^{d_{2k-1}} \phi_i''\phi_j''\,\mathrm{d}x + \sum_{k=1}^{p}(c_sI)_c \int_{d_{2k-1}}^{d_{2k}} \phi_i''\phi_j''\,\mathrm{d}x$$

$$K_{ij} = \sum_{k=1}^{p+1}(EI)_h \int_{d_{2k-2}}^{d_{2k-1}} \phi_i''\phi_j''\,\mathrm{d}x + \sum_{k=1}^{p}(EI)_c \int_{d_{2k-1}}^{d_{2k}} \phi_i''\phi_j''\,\mathrm{d}x \tag{8}$$

and the control influence matrix of voltage v_k on mode i is

$$D_{ik} = C_p[\phi_i'(d_{2k}) - \phi_i'(d_{2k-1})]$$

Equation (7) along with Eq. (8) are appropriate for any beam boundary conditions. Moreover, the model considers the mass and the stiffness of the piezoelectric patches. If the assumed mode functions $\phi_i(x)$ are judiciously chosen, better accuracy and more efficient convergence can be obtained.[21] Candidate functions are the mode shape functions of a uniform beam, which are available in the literature for all boundary conditions.

Measure of Modal Controllability and Observability

The second-order system given by Eq. (7) can be easily written as a first-order system

$$\dot{X} = AX + Bv(t) \tag{9}$$

where

$$X = \begin{pmatrix} q \\ \dot{q} \end{pmatrix}, \qquad A = \begin{bmatrix} 0 & I \\ -M^{-1}K & -M^{-1}C \end{bmatrix}, \qquad B = \begin{pmatrix} 0 \\ M^{-1}D \end{pmatrix} \tag{10}$$

Unlike the Popov, Belevitch, and Hautus (PBH) controllability test (see Ref. 22), which gives binary (yes/no) information, Hamdan and Nayfeh[22] proposed a measure of modal controllability/observabilty that reveals information on how controllable/observable each mode is for each actuator/sensor. This measure exploits the angles between the normalized left eigenvectors R_i of the system matrix A and the control input influence matrix B. The measure of controllability of the ith mode by the jth actuator is

$$\cos\theta_{ij} = \frac{\left|R_i^T b_j\right|}{\|R_i\|\|b_j\|} \tag{11}$$

with the magnitude notation $|\cdot|$ equal to the magnitude of $\cdot$ and $\|\cdot\|$ equal to the Euclidean (root-sum-square) norm of $\cdot$, where $R_i^T P_j = \delta_{ij}$ and b_j is the jth column vector of matrix B. If the angle θ_{ij} is equal to zero, the maximum controllability of mode i by actuator j is achieved. However, when the angle is 90 deg, the ith mode is uncontrollable by the jth actuator. The gross measure of controllability β_i of the ith mode by all actuators is given by the equation

$$\beta_i = \|f_i\| \tag{12a}$$

where

$$f_i^T = [\cos\theta_{i1}\|b_1\|, \cos\theta_{i2}\|b_2\|, \ldots, \cos\theta_{im}\|b_m\|] \tag{12b}$$

For a collocated system, note that the measure of modal controllability is equivalent to the measure of modal observability. More details and examples of the Hamdan and Nayfeh[22] measure may be found in Refs. 16, 21, and 22.

Measure of Modal Cost

Modal cost is defined as the contribution of the system's individual modes to the overall system response under a specific disturbance.[21] In other words, the modal cost can be interpreted as the relative importance of each system mode for a particular input. The disturbance can be introduced in the form of either initial conditions and/or an impulse force, both of which are widely used to study the transient response of the system. In this section, a brief review of the Skelton modal cost[21] is presented; this modal cost is based on unit impulse disturbance only.

The approximated equations of motion [Eq. (7)] of the stepped beam

$$M\ddot{q} + C\dot{q} + Kq = D_w u \tag{13}$$

can be modified to fit the modal cost analysis. Here M and K are given in Eq. (8) and D_w is the disturbance influence matrix. In line with standard practice, Rayleigh damping is assumed to avoid modal coupling caused by the damping.[23] It will be assumed that $c_s = aE$ and, thus, $C = aK$. Furthermore, because the modal cost is based on unit impulse disturbance, $\boldsymbol{u}$ is the unit impulse input. Here, $\boldsymbol{u}$ is a vector that permits application of an impulse disturbance at one of m locations. Equation (13) can be transformed into modal coordinates by introducing the normalized modal matrix Φ of M and K and the modal coordinates vector $\boldsymbol{\eta}(t)$ as follows.

Let $q(t) = \Phi\boldsymbol{\eta}(t)$; this leads to

$$\tilde{M}\ddot{\boldsymbol{\eta}} + \tilde{C}\dot{\boldsymbol{\eta}} + \tilde{K}\boldsymbol{\eta} = \tilde{D}_w\boldsymbol{u} \tag{14}$$

where the transformed (modal coordinates) mass, damping, stiffness, and disturbance influence matrices are, respectively, given by

$$\tilde{M} = \Phi^T M\Phi = I$$

$$\tilde{C} = \Phi^T C\Phi = \mathrm{diag}(2\zeta_1\omega_1, 2\zeta_1\omega_1, \ldots, 2\zeta_n w_n), \qquad \zeta_i = a\omega_i/2$$

$$\tilde{K} = \Phi^T K\Phi = \mathrm{diag}\left(\omega_1^2, \omega_2^2, \ldots, \omega_n^2\right), \qquad \tilde{D}_w = \Phi^T D_w$$

The system modal cost is evaluated by considering a cost function that represents the performance of the system. For m unit impulses, the cost function is given by

$$V = \sum_{i=1}^{m}\int_0^\infty y_d^{i^T}(t)Q_V y_d^i(t)\,\mathrm{d}t \tag{15}$$

where the output response $y_d(t)$ due to the unit impulse input $u_i(t)$ is expressed as

$$y_d(t) = \begin{bmatrix} C_{dx} & 0 \\ 0 & C_{d\dot{x}} \end{bmatrix}\begin{Bmatrix} q(t) \\ \dot{q}(t) \end{Bmatrix} = \begin{bmatrix} C_{dx}\Phi & 0 \\ 0 & C_{d\dot{x}}\Phi \end{bmatrix}\begin{Bmatrix} \eta(t) \\ \dot{\eta}(t) \end{Bmatrix} \tag{16}$$

These matrices can be chosen so that the cost function V becomes a meaningful physical quantity. For example, V can represent the kinetic and the potential energies of the system if $C_{dx} = C_{d\dot{x}} = \Phi^T$ and

$$Q_V = \begin{bmatrix} \mathrm{diag}\left(\omega_1^2, \omega_2^2, \ldots, \omega_n^2\right) & 0 \\ 0 & I \end{bmatrix}$$

are assigned. Other possible choices can be taken to have a cost function of importance to the designer.

The ith modal cost combines two parts; namely, the modal cost of the mode's displacement and the modal cost of the mode's velocity, and it is expressed as[21]

$$V_i = V_{\eta_i} + V_{\dot{\eta}_i} \tag{17}$$

where the modal cost of the ith mode's displacement and velocity are given by the equations

$$V_{\eta_i} = \left[X_{\eta\eta}\Phi^T C_{dx}^T Q_x C_{dx}\Phi\right]_{ii}, \qquad V_{\dot{\eta}_i} = \left[X_{\dot{\eta}\dot{\eta}}\Phi^T C_{d\dot{x}}^T Q_{\dot{x}} C_{d\dot{x}}\Phi\right]_{ii}$$

respectively, where

$$\begin{bmatrix} Q_x & 0 \\ 0 & Q_{\dot{x}} \end{bmatrix} = Q_V, \qquad [X_{\eta\eta}]_{ij} = \frac{2(\zeta_i\omega_i + \zeta_j\omega_j)}{\Delta}\left[\tilde{D}_w\tilde{D}_w^T\right]_{ij}$$

$$[X_{\dot{\eta}\dot{\eta}}]_{ij} = \frac{2\omega_i\omega_j(\zeta_i\omega_i + \zeta_j\omega_j)}{\Delta}\left[\tilde{D}_w\tilde{D}_w^T\right]_{ij}$$

$$\Delta = \left(\omega_i^2 - \omega_j^2\right)^2 + 4\omega_i\omega_j(\zeta_i\omega_i + \zeta_j\omega_j)(\zeta_i\omega_j + \zeta_j\omega_i)$$

Equation (17) represents the ith mode contribution to the total system cost from a unit impulse disturbance at location(s) that are specified in the disturbance influence matrix D_w. The disturbance would be at locations at the ends of the piezoelectric patches and would be in a moment form if $D_w = D$ is assigned.

Optimization Criterion

An attractive optimization criterion for actuator size and placement is based on the degree of modal controllability. The piezoelectric self-sensing actuator should be sized and placed to produce the maximum controllability/observability for all modes; however, it is impossible to find such size and location. Fortunately, in practice not all modes are of equal importance to the system response; the contribution of some modes is negligible. Therefore, there is no need to weight the less significant modes equal to the dominant ones. (Of course, because system response relates input and output, the modes to be neglected are configuration dependent.) The modal cost that was presented in the preceding section is a practical method to rank each mode's participation in the total system output. Kim and Junkins[16] proposed a controllability index given by

$$\alpha = \sum_{i=1}^{n} \frac{V_i}{V}\beta_i^2$$

The gross measure of controllability β_i is always positive and less than one; hence, squaring it seems unnecessary. The Kim and Junkins controllability index is modified by removing the square power of β_i to formulate the following optimization problem.

Determine the locations $d_k (k = 1, 2, \ldots, 2p)$ (see Fig. 1) that maximize the weighted controllability of the system's modes. This is mathematically written as

$$\begin{aligned} &\text{maximize} && \text{obj} = \alpha = \sum_{i=1}^{n} \frac{V_i}{V}\beta_i \\ &\text{subject to} && d_k - d_{k+1} < 0, \qquad d_{2p} - L \le 0 \\ &&& d_1, d_2, \ldots, d_{2p+1} \ge 0 \end{aligned} \tag{18}$$

where β_i, V, and V_i are given by Eqs. (12), (15), and (17), respectively. L, d_k, and d_{k+1}, in order, are the length of the beam, the distances from the left boundary of the beam to the left end and to the right end of the kth piezoelectric patch (Fig. 1). If the modal weight is known from any other weighting method, these weights may be used to replace the modal cost in Eq. (18).

Note that in the optimization problem (18) there was no restriction on the length of the actuator. This usually leads to practically infeasible actuator length (heavy, too long, very expensive, etc.). To design a practically realistic actuator size, the patch length should be constrained by adding a penalty term to the objective function given by Eq. (18). (It is also possible to limit the actuator size directly through a constraint on the maximum length.) The new proposed objective function is expressed as

$$\text{obj} = \alpha - \text{penalty} \tag{19}$$

By judicious selection (design dependent) of the penalty, a practically reasonable patch length can be obtained. For the sake of demonstration, the penalty term is chosen such that the objective function reduces drastically in a quadratic manner when the length of each patch exceeds a particular fraction of the beam length:

$$\text{obj} = \alpha - \sum_{k=1}^{p}\left(\frac{d_{2k} - d_{2k-1}}{\gamma L}\right)^2 \tag{20}$$

where γ is a scaling fraction, $0 < \gamma < 1$. Equation (18) as well as Eq. (20) will be employed in the next section.

Numerical Examples

The optimal length and location of piezoelectric actuators are determined for a number of beam boundary conditions: free–free, clamped–free, clamped–pinned, clamped–sliding, clamped–clamped, and pinned–pinned beams (Fig. 2). A five-mode model is used to approximate the beam deflection. The assumed modes, $\phi_i(x)$ in Eq. (6), are chosen to be those of the uniform Euler–Bernoulli beams, which are available in many references (for example, see Inman[24]). The modal cost (weight) is calculated by using the method given in the "Measure of Modal Cost" section.

The disturbance matrix D_w and, thus, modal cost is sensitive to large changes in the location(s) of the unit impulse disturbance but not to small changes. Numerical calculations indicate approximately 11% change in the modal cost for a disturbance location change of $\pm 0.05L$. Therefore, the position(s) of the unit impulse disturbance should be assigned appropriately (in a problem-dependent manner) to reflect the expected system excitation. Once the optimal actuator parameters are obtained for a specific disturbance location, the objective function is relatively insensitive to the disturbance location if the location of the disturbance is in the vicinity of the one used in the optimization. As example, the pinned–pinned beam has a sensitivity of at most 4% in the objective function for a variation of $\pm 0.05L$ in the disturbance location. For illustration, the location of the impulse unit input is selected to excite the modeled modes of the beam; otherwise, it is chosen based on design requirements. The Q_v, C_{dx}, and $C_{d\dot{x}}$ matrices are chosen so that the modal cost represents the energy contribution of each mode.

We investigated two sets of beam examples: beams with one pair and beams with two pairs of piezoelectric actuators. In all examples, the actuators are piezoceramic PZT-4 patches that are attached on an aluminum host beam of length $L = 0.5$ m. The beam and the patches are of equal width, $b = 5$ mm, and have thickness $t_h = 1$ mm and $t_p = 0.1$ mm. The internal modal damping factor of the beam is assumed to be $\xi = 0.001$ for all modes.[21] The properties of the aluminum host beam and of the piezoelectric patches are as follows. For the Al beam, the density $\rho_h = 2840$ kg/m^3 and Young's modulus $E_h = 76$ GPa. For the PZT-4 (Ref. 25), the density $\rho_p = 7500$ kg/m^3 and Young's modulus $E_p = 81.3$ GPa. The piezoelectric coefficient $d_{31} = -123 \times 10^{-12}$ m/V. In the interest of simplicity, only the length and the location of the patches are considered as the optimization

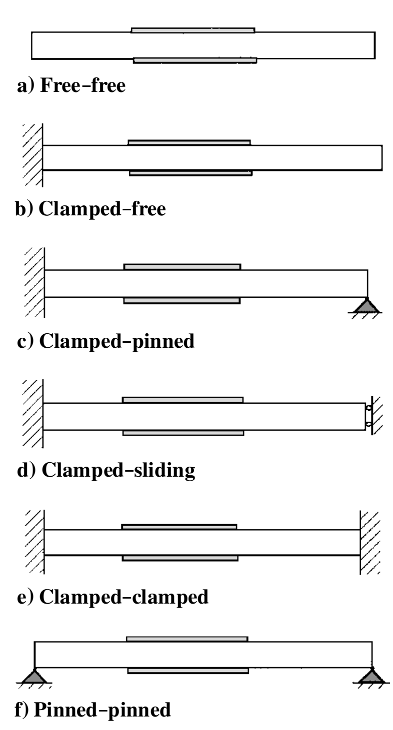

Fig. 2 Beam configurations.

Table 1 Optimization results of a beam with one pair of actuators for various boundary conditions

							Optimal results			
	Disturbance	Model cost at optimum, %					Equation (18)		Equation (20)	
Beam configuration	location	1st	2nd	3rd	4th	5th	$d1/L$	$d2/L$	$d1/L$	$d2/L$
Free–free	0.4L	65	18	6	9	1	0	0.79	0.29	0.83
Clamped–free	0.7L	78	9	10	2	1	0	1	0	0.6
Clamped–pinned	0.4L	67	25	0	7	1	0.36	1	0.37	0.92
Clamped–sliding	0.4L	49	41	2	4	4	0.06	0.67	0.36	0.75
Clamped–clamped	0.4L	70	20	2	8	0	0.3	1	0.32	0.84
Pinned–pinned	0.3L	72	22	1	2	3	0.25	1	0.23	0.49

Table 2 Optimization results of a beam with two pairs of actuators for various boundary conditions

		Optimal results							
	Disturbance	Equation (20)				Equation (18)			
Beam configuration	location	$d1/L$	$d2/L$	$d3/L$	$d4/L$	$d1/L$	$d2/L$	$d3/L$	$d4/L$
Free–free	0.4L	0.149	0.677	0.677	0.85	0.046	0.735	0.735	0.985
Clamped–free	0.7L	0	0.535	0.58	0.79	0	0.95	0.95	1
Clamped–pinned	0.4L	0.27	0.45	0.45	0.91	0	0.39	0.39	1
Clamped–sliding	0.4L	0.3	0.62	0.67	1	0.159	0.65	0.65	1
Clamped–clamped	0.4L	0	0.15	0.56	0.65	0.06	0.27	0.27	1
Pinned–pinned	0.3L	0.12	0.43	0.43	0.89	0	0.46	0.46	1

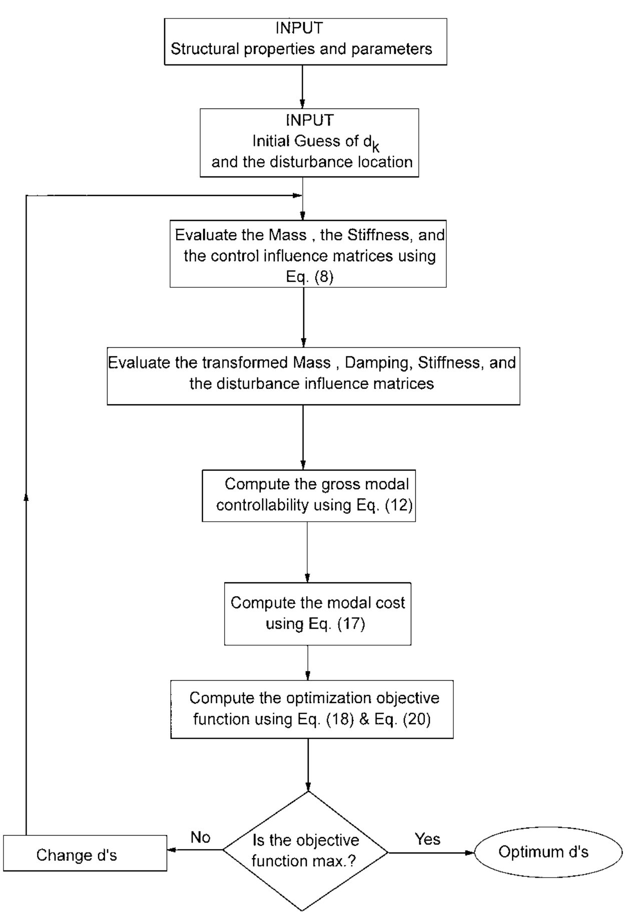

Fig. 3 Flowchart of the optimization process.

parameters. If they are of interest, other parameters such as the width and the thickness can be easily introduced into the optimization problem.

The flowchart for finding the optimal parameters d_k and d_{k+1} is given in Fig. 3. Tables 1 and 2 show the optimal results of one and two pairs, respectively, of patches for beams with different boundary conditions. The modal costs for the various modes change during the optimizations because the mass and stiffness of the actuator alter the modes. In Table 1, we give the modal costs at the optimal point. Although the objective function that is given in Eq. (18) is not of practical importance, it is employed to predict the ideal optimal results and to compare the results of this paper with literature results, if available. The practically realistic objective function Eq. (20) is utilized for all beam cases, and its optimal results are also shown in Tables 1 and 2. The scaling fraction $\gamma = 0.25$ is selected such that the objective function reduces drastically when the length of the actuator exceeds 25% the length of the beam.

For one pair of actuators (Table 1), our optimal results of a clamped–free beam are identical to those of the overall damping criteria that are reported by Yousefi–Koma and Vukovich.[13] Furthermore, the results of pinned–pinned beam agree very well with those reported by Devasia et al.[10] For the other beam cases, there are no available results in the literature to compare with. Figures 4a–4f show surface plots of the objective function of the unconstrained patch length case for one pair of actuators. These plots are generated over the permissible domain of the independent variables, namely, $0 < d_1 < L$ and $d_1 < d_2 < L$. It is not unexpected that in the clamped–free case the optimal length is the beam length because the beam midpoint is not a node of any of the considered modes. For the free–free beam, the clamped–clamped beam, and the pinned–pinned beam, the beam midpoint is a node of the even modes; thus, it is avoided as an optimal center location for the patch although the longer the patch the higher the controllability of the odd modes.

For two pairs of patches, we found that the objective function is always higher than that for one pair of patches, indicating higher modal controllability than that generated by one actuator pair. However, the total length of the two pairs of patches is longer than that of one patch. In spite of increased length of the two pairs, there is a great gain in the modal controllability. Thus, for vibration control, it is recommended to utilize multiple pairs of short piezoelectric actuators instead of a single pair of a long actuators. Note that in Table 2 although the optimal locations of the two patches look as if they were a single patch, their control action is different than that of a single patch. The two patches can act in phase when their control voltage is in phase or can act out of phase when their control voltage is out of phase, permitting more control authority. In this manner, symmetric and antisymmetric modes can be controlled by in-phase and out-of-phase voltages, respectively.

The sensitivity of the optimization results to the mass and stiffness of the piezoelectric patches is investigated for the pinned–pinned beam with one pair of PZT patches. Table 3 shows the optimal results when the mass, the stiffness, or both are ignored. A comparison with the results of Table 1 is indicated in the error column. Although

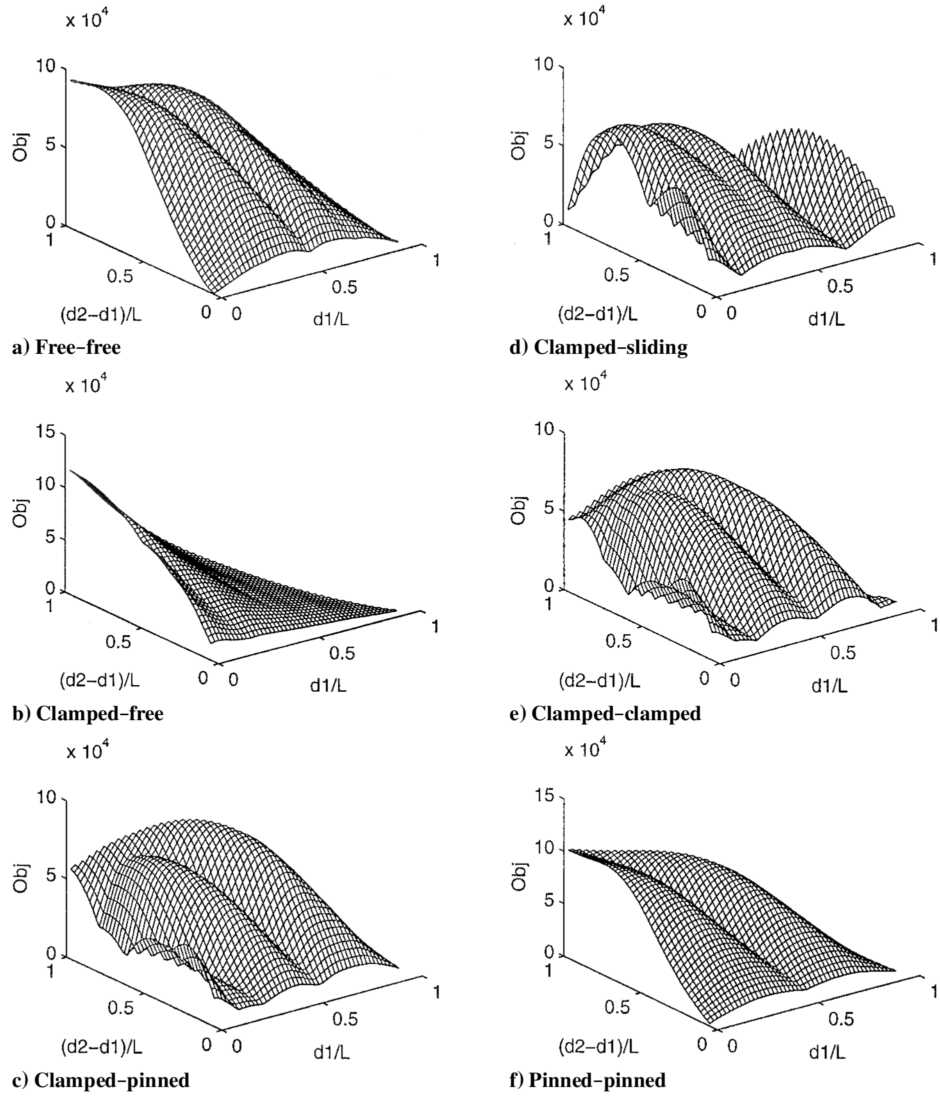

Fig. 4 Surface plot of the objective function of the unconstrained patch length for one pair of actuators.

Table 3 Optimization results of a pinned–pinned beam with one pair of actuators

	Equation (18)			Equation (20)		
Case	$d1/L$	$d2/L$	% error	$d1/L$	$d2/L$	% error
PZT mass ignored	0.26	1	2	0.24	0.5	4
PZT stiffness ignored	0.23	1	3	0.22	0.5	4
PZT mass and stiffness ignored	0.26	1	2	0.235	0.5	4
PZT mass and stiffness included	0.25	1	——	0.23	0.49	——

ignoring the mass and stiffness of PZT causes a small error in the results of the examples considered in this paper, their effects should not be neglected for relatively thick PZT patches.

Conclusions

We formulated an optimization criterion for actuator/sensor sizing and placement. Both the inertia and the stiffness of the piezoelectric patches are included in the model. The proposed criterion is controller independent and is based on practically realistic considerations. The modal costs (weights) are calculated for each mode of the flexible beam and are accordingly used to weight the modal controllability in the objective function. It has been shown that the length of the actuator can be penalized to achieve a practically reasonable actuator size. By comparing the results of two beam examples with other authors' results, we verified the validity as well as the accuracy of the criterion. A general procedure for the optimization of location and size of piezoelectric patches is presented considering all possible boundary conditions. It should be mentioned that the results in this paper are suitable for any beam problem with similar boundary conditions and with similar modal contributions.

The performance of a single pair and two pairs of actuators are then compared for several beam examples. The results showed that two pairs of actuators can control the vibration in beams more effectively than a single pair. It also suggests that using several short pairs of actuators is better than using one long pair, although this requires further confirmation.

References

[1]Tzou, H. S., and Anderson, G. L., *Intelligent Structural Systems*, Kluwer Academic, Norwell, MA, 1992, pp. 75–244.

[2]Crawley, E. F., and Anderson, E. H., "Detailed Models of Piezoelectric Actuation of Beams," *Journal of Intelligent Material Systems and Structures*, Vol. 1, Jan. 1990, pp. 4–25.

[3]Bailey, T., and Hubbard, J. E. Jr., "Distributed Piezoelectric-Polymer Active Vibration Control of a Cantilever Beam," *Journal of Guidance, Control, and Dynamics*, Vol. 8, No. 5, 1985, pp. 605–611.

[4]Lee, C. K., "Theory of Laminated Piezoelectric Plates for the Design of Distributed Sensors/Actuators. Part I: Governing Equations and Reciprocal Relationships," *Journal of the Acoustical Society of America*, Vol. 87, No. 3, 1990, pp. 1144–1158.

[5]Lee, C. K., "Piezoelectric Laminates for Torsional and Bending Modal Control: Theory and Experiment," Ph.D. Dissertation, Cornell Univ., Ithaca, NY, 1987.

[6]Shieh, R. C., "Governing Equations and Finite Element Models for Multiaxial Piezoelectric Beam Sensors/Actuators," *AIAA Journal*, Vol. 32, No. 6, 1994, pp. 1250–1258.

[7]Crawley, E. F., and de Luis, J., "Use of Piezoelectric Actuators as Elements of Intelligent Structures," *AIAA Journal*, Vol. 25, No. 10, 1985, pp. 1373–1385.

[8]Baz, A., and Poh, S., "Performance of an Active Control System with Piezoelectric Actuators," *Journal of Sound and Vibration*, Vol. 126, No. 2, 1988, pp. 327–343.

[9]Baz, A., and Poh, S., "Experimental Implementation of the Modified Independent Modal Space Control Method," *Journal of Sound and Vibration*, Vol. 139, No. 1, 1990, pp. 133–149.

[10]Devasia, S., Meressi, T., Paden, B., and Bayo, E., "Piezoelectric Actuator Design for Vibration Suppression: Placement and Sizing," *Journal of Guidance, Control, and Dynamics*, Vol. 16, No. 5, 1993, pp. 859–864.

[11]Burke, S. E., and Sullivan, J. M., "Distribution Transducer Shading via Spatial Gradient Electrodes," *Smart Structures and Materials 1995*, Vol. 2443, Society of Photo-Optical Instrumentation Engineers, 1995, pp. 716–726.

[12]Sunar, M., and Rao, S. S., "Distributed Modeling and Actuator Location for Piezoelectric Control Systems," *AIAA Journal*, Vol. 34, No. 10, 1996, pp. 2209–2211.

[13]Yousefi-Koma, A., and Vukovich, A., "Shape and Location Optimization of Piezoelectric Actuators in Active Control System," *Proceeding of the ASME Aerospace Division*, AD-Vol. 52, American Society of Mechanical Engineers, Fairfield, NJ, 1996, pp. 559–566.

[14]Gabbert, U., and Schulz, I., "On Optimal Placement of Piezoelectric Actuators in Vibration Control of Adaptive Structures," *Proceeding of the ASME Active Control of Vibration and Noise*, AD-Vol. 93, American Society of Mechanical Engineers, Fairfield, NJ, 1996, pp. 271–277.

[15]Yang, S. M., and Lee, Y. J., "Modal Analysis of Stepped Beams with Piezoelectric Materials," *Journal of Sound and Vibration*, Vol. 176, No. 3, 1994, pp. 289–300.

[16]Kim, Y., and Junkins, J. L., "Measure of Controllability for Actuator Placement," *Journal of Guidance, Control, and Dynamics*, Vol. 14, No. 5, 1991, pp. 895–902.

[17]Dosch, J. J., Inman, D. J., and Garcia, E., "A Self-Sensing Piezoelectric Actuator for Collocated Control," *Journal of Intelligent Material Systems and Structures*, Vol. 3, Jan. 1992, pp. 166–185.

[18]Vipperman, J. S., and Clark, R. L., "Implementation of an Adaptive Piezoelectric Sensoriactuator," *AIAA Journal*, Vol. 34, No. 10, 1996, pp. 2102–2109.

[19]Clough, R. W., and Penzien, J., *Dynamics of Structures*, McGraw–Hill, New York, 1975, pp. 369, 370.

[20]Meirovitch, L., *Elements of Vibration Analysis*, McGraw–Hill, New York, 1986, pp. 282–285.

[21]Junkins, J. L., and Kim, Y., *Introduction to Dynamics and Control of Flexible Structures*, AIAA, Washington, DC, 1993, pp. 315–330.

[22]Hamdan, A. M. A., and Nayfeh, A. H., "Measure of Controllability and Observability for First- and Second-Order Linear Systems," *Journal of Guidance, Control, and Dynamics*, Vol. 12, No. 3, 1989, pp. 421–428.

[23]Thomson, W. T., *Theory of Vibrations with Applications*, 4th ed., Prentice–Hall, Englewood Cliffs, NJ, 1993, pp. 175–177.

[24]Inman, D. J., *Engineering Vibration*, Prentice–Hall, Englewood Cliffs, NJ, 1996, pp. 329–340.

[25]*Data For Designers*, Electro Ceramic Div., Morgan Matroc, Inc., Bedford, OH.